Search for s-Channel Single-Top-Quark Production in Events with Missing Energy Plus Jets in $p\bar{p}$ Collisions at $\sqrt{s} = 1.96$ TeV

T. Aaltonen,[21] S. Amerio,[39a,39b] D. Amidei,[31] A. Anastassov,[15,w] A. Annovi,[17] J. Antos,[12] G. Apollinari,[15] J. A. Appel,[15] T. Arisawa,[52] A. Artikov,[13] J. Asaadi,[47] W. Ashmanskas,[15] B. Auerbach,[2] A. Aurisano,[47] F. Azfar,[38] W. Badgett,[15] T. Bae,[25] A. Barbaro-Galtieri,[26] V. E. Barnes,[43] B. A. Barnett,[23] P. Barria,[41a,41c] P. Bartos,[12] M. Bauce,[39a,39b] F. Bedeschi,[41a] S. Behari,[15] G. Bellettini,[41a,41b] J. Bellinger,[54] D. Benjamin,[14] A. Beretvas,[15] A. Bhatti,[45] K. R. Bland,[5] B. Blumenfeld,[23] A. Bocci,[14] A. Bodek,[44] D. Bortoletto,[43] J. Boudreau,[42] A. Boveia,[11] L. Brigliadori,[6b] C. Bromberg,[32] E. Brucken,[21] J. Budagov,[13] H. S. Budd,[44] K. Burkett,[15] G. Busetto,[39a,39b] P. Bussey,[19] P. Butti,[41a,41b] A. Buzatu,[19] A. Calamba,[10] S. Camarda,[4] M. Campanelli,[28] F. Canelli,[11,dd] B. Carls,[22] D. Carlsmith,[54] R. Carosi,[41a] S. Carrillo,[16,m] B. Casal,[9,k] M. Casarsa,[48a] A. Castro,[6a] P. Catastini,[20] D. Cauz,[48a,48b,48c] V. Cavaliere,[22] M. Cavalli-Sforza,[4] A. Cerri,[26,f] L. Cerrito,[28,r] Y. C. Chen,[1] M. Chertok,[7] G. Chiarelli,[41a] G. Chlachidze,[15] K. Cho,[25] D. Chokheli,[13] A. Clark,[18] C. Clarke,[53] M. E. Convery,[15] J. Conway,[7] M. Corbo,[15,z] M. Cordelli,[17] C. A. Cox,[7] D. J. Cox,[7] M. Cremonesi,[41a] D. Cruz,[47] J. Cuevas,[9,y] R. Culbertson,[15] N. d'Ascenzo,[15,v] M. Datta,[15,gg] P. de Barbaro,[44] L. Demortier,[45] M. Deninno,[6a] M. D'Errico,[39a,39b] F. Devoto,[21] A. Di Canto,[41a,41b] B. Di Ruzza,[15,q] J. R. Dittmann,[5] S. Donati,[41a,41b] M. D'Onofrio,[27] M. Dorigo,[48a,48d] A. Driutti,[48a,48b,48c] K. Ebina,[52] R. Edgar,[31] A. Elagin,[47] R. Erbacher,[7] S. Errede,[22] B. Esham,[22] S. Farrington,[38] J. P. Fernández Ramos,[29] R. Field,[16] G. Flanagan,[15,t] R. Forrest,[7] M. Franklin,[20] J. C. Freeman,[15] H. Frisch,[11] Y. Funakoshi,[52] C. Galloni,[41a,41b] A. F. Garfinkel,[43] P. Garosi,[41a,41c] H. Gerberich,[22] E. Gerchtein,[15] S. Giagu,[46a] V. Giakoumopoulou,[3] K. Gibson,[42] C. M. Ginsburg,[15] N. Giokaris,[3] P. Giromini,[17] G. Giurgiu,[23] V. Glagolev,[13] D. Glenzinski,[15] M. Gold,[34] D. Goldin,[47] A. Golossanov,[15] G. Gomez,[9] G. Gomez-Ceballos,[30] M. Goncharov,[30] O. González López,[29] I. Gorelov,[34] A. T. Goshaw,[14] K. Goulianos,[45] E. Gramellini,[6a] S. Grinstein,[4] C. Grosso-Pilcher,[11] R. C. Group,[51,15] J. Guimaraes da Costa,[20] S. R. Hahn,[15] J. Y. Han,[44] F. Happacher,[17] K. Hara,[49] M. Hare,[50] R. F. Harr,[53] T. Harrington-Taber,[15,n] K. Hatakeyama,[5] C. Hays,[38] J. Heinrich,[40] M. Herndon,[54] A. Hocker,[15] Z. Hong,[47] W. Hopkins,[15,g] S. Hou,[1] R. E. Hughes,[35] U. Husemann,[55] M. Hussein,[32,bb] J. Huston,[32] G. Introzzi,[41a,41e,41f] M. Iori,[46a,46b] A. Ivanov,[7,p] E. James,[15] D. Jang,[10] B. Jayatilaka,[15] E. J. Jeon,[25] S. Jindariani,[15] M. Jones,[43] K. K. Joo,[25] S. Y. Jun,[10] T. R. Junk,[15] M. Kambeitz,[24] T. Kamon,[25,47] P. E. Karchin,[53] A. Kasmi,[5] Y. Kato,[37,o] W. Ketchum,[11,hh] J. Keung,[40] B. Kilminster,[15,dd] D. H. Kim,[25] H. S. Kim,[25] J. E. Kim,[25] M. J. Kim,[17] S. H. Kim,[49] S. B. Kim,[25] Y. J. Kim,[25] Y. K. Kim,[11] N. Kimura,[52] M. Kirby,[15] K. Knoepfel,[15] K. Kondo,[52,a] D. J. Kong,[25] J. Konigsberg,[16] A. V. Kotwal,[14] M. Kreps,[24] J. Kroll,[40] M. Kruse,[14] T. Kuhr,[24] M. Kurata,[49] A. T. Laasanen,[43] S. Lammel,[15] M. Lancaster,[28] K. Lannon,[35,x] G. Latino,[41a,41c] H. S. Lee,[25] J. S. Lee,[25] S. Leo,[41a] S. Leone,[41a] J. D. Lewis,[15] A. Limosani,[14,s] E. Lipeles,[40] A. Lister,[18,b] H. Liu,[51] Q. Liu,[43] T. Liu,[15] S. Lockwitz,[55] A. Loginov,[55] D. Lucchesi,[39a,39b] A. Lucà,[17] J. Lueck,[24] P. Lujan,[26] P. Lukens,[15] G. Lungu,[45] J. Lys,[26] R. Lysak,[12,e] R. Madrak,[15] P. Maestro,[41a,41c] S. Malik,[45] G. Manca,[27,c] A. Manousakis-Katsikakis,[3] L. Marchese,[6a,ii] F. Margaroli,[46a] P. Marino,[41a,41d] M. Martínez,[4] K. Matera,[22] M. E. Mattson,[53] A. Mazzacane,[15] P. Mazzanti,[6a] R. McNulty,[27,j] A. Mehta,[27] P. Mehtala,[21] C. Mesropian,[45] T. Miao,[15] D. Mietlicki,[31] A. Mitra,[1] H. Miyake,[49] S. Moed,[15] N. Moggi,[6a] C. S. Moon,[15,z] R. Moore,[15,ee,ff] M. J. Morello,[41a,41d] A. Mukherjee,[15] Th. Muller,[24] P. Murat,[15] M. Mussini,[6a] J. Nachtman,[15,n] Y. Nagai,[49] J. Naganoma,[52] I. Nakano,[36] A. Napier,[50] J. Nett,[47] C. Neu,[51] T. Nigmanov,[42] L. Nodulman,[2] S. Y. Noh,[25] O. Norniella,[22] L. Oakes,[38] S. H. Oh,[14] Y. D. Oh,[25] I. Oksuzian,[51] T. Okusawa,[37] R. Orava,[21] L. Ortolan,[4] C. Pagliarone,[48a] E. Palencia,[9,f] P. Palni,[34] V. Papadimitriou,[15] W. Parker,[54] G. Pauletta,[48a,48b,48c] M. Paulini,[10] C. Paus,[30] T. J. Phillips,[14] G. Piacentino,[41a] E. Pianori,[40] J. Pilot,[7] K. Pitts,[22] C. Plager,[8] L. Pondrom,[54] S. Poprocki,[15,g] K. Potamianos,[26] A. Pranko,[26] F. Prokoshin,[13,aa] F. Ptohos,[17,h] G. Punzi,[41a,41b] N. Ranjan,[43] I. Redondo Fernández,[29] P. Renton,[38] M. Rescigno,[46a] F. Rimondi,[6a,a] L. Ristori,[41a,15] A. Robson,[19] T. Rodriguez,[40] S. Rolli,[50,I] M. Ronzani,[41a,41b] R. Roser,[15] J. L. Rosner,[11] F. Ruffini,[41a,41c] A. Ruiz,[9] J. Russ,[10] V. Rusu,[15] W. K. Sakumoto,[44] Y. Sakurai,[52] L. Santi,[48a,48b,48c] K. Sato,[49] V. Saveliev,[15,v] A. Savoy-Navarro,[15,z] P. Schlabach,[15] E. E. Schmidt,[15] T. Schwarz,[31] L. Scodellaro,[9] F. Scuri,[41a] S. Seidel,[34] Y. Seiya,[37] A. Semenov,[13] F. Sforza,[41a,41b] S. Z. Shalhout,[7] T. Shears,[27] P. F. Shepard,[42] M. Shimojima,[49,u] M. Shochet,[11] I. Shreyber-Tecker,[33] A. Simonenko,[13] K. Sliwa,[50] J. R. Smith,[7] F. D. Snider,[15] H. Song,[42] V. Sorin,[4] R. St. Denis,[19] M. Stancari,[15] D. Stentz,[15,w] J. Strologas,[34] Y. Sudo,[49] A. Sukhanov,[15] I. Suslov,[13] K. Takemasa,[49] Y. Takeuchi,[49] J. Tang,[11] M. Tecchio,[31] P. K. Teng,[1] J. Thom,[15,g] E. Thomson,[40] V. Thukral,[47] D. Toback,[47] S. Tokar,[12] K. Tollefson,[32] T. Tomura,[49] D. Tonelli,[15,f] S. Torre,[17] D. Torretta,[15] P. Totaro,[39a] M. Trovato,[41a,41d] F. Ukegawa,[49] S. Uozumi,[25] G. Velev,[15] C. Vellidis,[15] C. Vernieri,[41a,41d] M. Vidal,[43] R. Vilar,[9] J. Vizán,[9,cc] M. Vogel,[34] G. Volpi,[17] F. Vázquez,[16,m] P. Wagner,[40] R. Wallny,[15,k] S. M. Wang,[1] D. Waters,[28] W. C. Wester III,[15] D. Whiteson,[40,d] A. B. Wicklund,[2]

S. Wilbur,[7] H. H. Williams,[40] J. S. Wilson,[31] P. Wilson,[15] B. L. Winer,[35] P. Wittich,[15,g] S. Wolbers,[15] H. Wolfe,[35] T. Wright,[31] X. Wu,[18] Z. Wu,[5] K. Yamamoto,[37] D. Yamato,[37] T. Yang,[15] U. K. Yang,[25] Y. C. Yang,[25] W.-M. Yao,[26] G. P. Yeh,[15] K. Yi,[15,n] J. Yoh,[15] K. Yorita,[52] T. Yoshida,[37,l] G. B. Yu,[14] I. Yu,[25] A. M. Zanetti,[48a] Y. Zeng,[14] C. Zhou,[14] and S. Zucchelli[6b]
(CDF Collaboration)

[1]*Institute of Physics, Academia Sinica, Taipei, Taiwan 11529, Republic of China*
[2]*Argonne National Laboratory, Argonne, Illinois 60439, USA*
[3]*University of Athens, 157 71 Athens, Greece*
[4]*Institut de Fisica d'Altes Energies, ICREA, Universitat Autonoma de Barcelona, E-08193, Bellaterra (Barcelona), Spain*
[5]*Baylor University, Waco, Texas 76798, USA*
[6a]*Istituto Nazionale di Fisica Nucleare Bologna, Italy*
[6b]*University of Bologna, I-40127 Bologna, Italy*
[7]*University of California, Davis, Davis, California 95616, USA*
[8]*University of California, Los Angeles, Los Angeles, California 90024, USA*
[9]*Instituto de Fisica de Cantabria, CSIC-University of Cantabria, 39005 Santander, Spain*
[10]*Carnegie Mellon University, Pittsburgh, Pennsylvania 15213, USA*
[11]*Enrico Fermi Institute, University of Chicago, Chicago, Illinois 60637, USA*
[12]*Comenius University, 842 48 Bratislava, Slovakia; Institute of Experimental Physics, 040 01 Kosice, Slovakia*
[13]*Joint Institute for Nuclear Research, RU-141980 Dubna, Russia*
[14]*Duke University, Durham, North Carolina 27708, USA*
[15]*Fermi National Accelerator Laboratory, Batavia, Illinois 60510, USA*
[16]*University of Florida, Gainesville, Florida 32611, USA*
[17]*Laboratori Nazionali di Frascati, Istituto Nazionale di Fisica Nucleare, I-00044 Frascati, Italy*
[18]*University of Geneva, CH-1211 Geneva 4, Switzerland*
[19]*Glasgow University, Glasgow G12 8QQ, United Kingdom*
[20]*Harvard University, Cambridge, Massachusetts 02138, USA*
[21]*Division of High Energy Physics, Department of Physics, University of Helsinki, FIN-00014, Helsinki, Finland; Helsinki Institute of Physics, FIN-00014, Helsinki, Finland*
[22]*University of Illinois, Urbana, Illinois 61801, USA*
[23]*The Johns Hopkins University, Baltimore, Maryland 21218, USA*
[24]*Institut für Experimentelle Kernphysik, Karlsruhe Institute of Technology, D-76131 Karlsruhe, Germany*
[25]*Center for High Energy Physics: Kyungpook National University, Daegu 702-701, Korea; Seoul National University, Seoul 151-742, Korea; Sungkyunkwan University, Suwon 440-746, Korea; Korea Institute of Science and Technology Information, Daejeon 305-806, Korea; Chonnam National University, Gwangju 500-757, Korea; Chonbuk National University, Jeonju 561-756, Korea; Ewha Womans University, Seoul 120-750, Korea*
[26]*Ernest Orlando Lawrence Berkeley National Laboratory, Berkeley, California 94720, USA*
[27]*University of Liverpool, Liverpool L69 7ZE, United Kingdom*
[28]*University College London, London WC1E 6BT, United Kingdom*
[29]*Centro de Investigaciones Energeticas Medioambientales y Tecnologicas, E-28040 Madrid, Spain*
[30]*Massachusetts Institute of Technology, Cambridge, Massachusetts 02139, USA*
[31]*University of Michigan, Ann Arbor, Michigan 48109, USA*
[32]*Michigan State University, East Lansing, Michigan 48824, USA*
[33]*Institution for Theoretical and Experimental Physics, ITEP, Moscow 117259, Russia*
[34]*University of New Mexico, Albuquerque, New Mexico 87131, USA*
[35]*The Ohio State University, Columbus, Ohio 43210, USA*
[36]*Okayama University, Okayama 700-8530, Japan*
[37]*Osaka City University, Osaka 558-8585, Japan*
[38]*University of Oxford, Oxford OX1 3RH, United Kingdom*
[39a]*Istituto Nazionale di Fisica Nucleare, Sezione di Padova, Italy*
[39b]*University of Padova, I-35131 Padova, Italy*
[40]*University of Pennsylvania, Philadelphia, Pennsylvania 19104, USA*
[41a]*Istituto Nazionale di Fisica Nucleare Pisa, Italy*
[41b]*University of Pisa, Italy*
[41c]*University of Siena, Italy*
[41d]*Scuola Normale Superiore, I-56127 Pisa, Italy*
[41e]*INFN Pavia, I-27100 Pavia, Italy*
[41f]*University of Pavia, I-27100 Pavia, Italy*
[42]*University of Pittsburgh, Pittsburgh, Pennsylvania 15260, USA*
[43]*Purdue University, West Lafayette, Indiana 47907, USA*

[44]University of Rochester, Rochester, New York 14627, USA
[45]The Rockefeller University, New York, New York 10065, USA
[46a]Istituto Nazionale di Fisica Nucleare, Sezione di Roma 1, Italy
[46b]Sapienza Università di Roma, I-00185 Roma, Italy
[47]Mitchell Institute for Fundamental Physics and Astronomy, Texas A&M University, College Station, Texas 77843, USA
[48a]Istituto Nazionale di Fisica Nucleare Trieste, Italy
[48b]Gruppo Collegato di Udine, Italy
[48c]University of Udine, I-33100 Udine, Italy
[48d]University of Trieste, I-34127 Trieste, Italy
[49]University of Tsukuba, Tsukuba, Ibaraki 305, Japan
[50]Tufts University, Medford, Massachusetts 02155, USA
[51]University of Virginia, Charlottesville, Virginia 22906, USA
[52]Waseda University, Tokyo 169, Japan
[53]Wayne State University, Detroit, Michigan 48201, USA
[54]University of Wisconsin, Madison, Wisconsin 53706, USA
[55]Yale University, New Haven, Connecticut 06520, USA
(Received 21 February 2014; published 9 June 2014)

The first search for single-top-quark production from the exchange of an s-channel virtual W boson using events with an imbalance in the total transverse energy, b-tagged jets, and no identified leptons is presented. Assuming the electroweak production of top quarks of mass 172.5 GeV/c^2 in the s channel, a cross section of $1.12^{+0.61}_{-0.57}$ (stat + syst) pb with a significance of 1.9 standard deviations is measured. This measurement is combined with the result obtained from events with an imbalance in total transverse momentum, b-tagged jets, and exactly one identified lepton, yielding a cross section of $1.36^{+0.37}_{-0.32}$ (stat + syst) pb, with a significance of 4.2 standard deviations.

DOI: 10.1103/PhysRevLett.112.231805 PACS numbers: 14.65.Ha, 12.15.Ji, 13.85.Ni

The top quark was discovered at Fermilab in 1995 [1,2] through top-antitop-quark-pair production. This process is mediated by the strong interaction and results in the largest contribution to the top-quark-production cross section in hadron colliders. The top quark can also be produced singly via the electroweak interaction involving the Wtb vertex with a W boson and a b quark. The study of single-top-quark production is particularly interesting because of the direct dependence of the cross section on the magnitude of the Wtb coupling. Furthermore, electroweak single-top-quark production from the exchange of an s-channel virtual W boson is of special interest since possible deviations from the standard model (SM) expectation could indicate evidence for non-SM particles such as higher-mass partners of the W boson (W') or charged Higgs bosons [3]. Examples of SM single-top-quark-production processes dominating at the Tevatron are shown in Fig. 1.

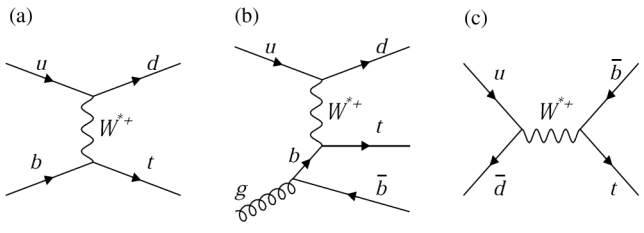

FIG. 1. Feynman diagrams for electroweak single-top-quark production: (a) leading-order t channel, (b) next-to-leading-order t channel, and (c) leading-order s channel.

Single-top-quark production was observed at the Tevatron in 2009 [4–6]. However, s-channel production has yet to be observed independently. While single-top-quark production through the t-channel exchange of a W boson, first observed by the D0 experiment [7], was established in Large Hadron Collider (LHC) proton-proton collisions [8,9], the s-channel process has an unfavorable production rate compared to the background rates at the LHC. The D0 Collaboration reported the first evidence of s-channel single-top-quark production [10] measuring a cross section of $1.10^{+0.33}_{-0.31}$ (stat + syst) pb, with a significance of 3.7 standard deviations. More recently, CDF also obtained 3.8 standard deviation evidence using events containing one isolated muon or electron, large missing transverse energy ($\not\!\!E_T$) [11], and two jets, at least one of which is identified as likely to have originated from a bottom quark (b tagged) [12]. This sample is referred to as the $\ell\nu b\bar{b}$ sample. To add acceptance to the data set with identified leptons, CDF uses, for the first time, events with large $\not\!\!E_T$, two or three jets of which one or more are b tagged and no detected electron or muon candidates. This sample of events is referred to as the $\not\!\!E_T b\bar{b}$ sample and contains s-channel single-top-quark contributions where $t \to Wb \to \ell\nu$ and ℓ is an electron or a muon that is not identified in the detector or a tau that decays hadronically. In this Letter, the search for s-channel single-top-quark production in the $\not\!\!E_T b\bar{b}$ sample is reported. Most of the techniques developed for the low-mass Higgs boson search [13] in the same data sample are exploited, including the

HOBIT b tagger [14]. By combining the results of the two searches, an improved sensitivity to s-channel single top production from the 9.45 fb^{-1} of integrated luminosity from the full CDF II data set is obtained.

In the $E_T b\bar{b}$ analysis, events are accepted by the online event selection (trigger) that requires $\not\!\!E_T > 45$ GeV or, alternatively, $\not\!\!E_T > 35$ GeV and two or more jets with transverse energy $E_T > 15$ GeV. The efficiency associated with this selection is obtained from data and is applied to the Monte Carlo simulated samples to reproduce the efficiencies of the data. The parametrization of the trigger efficiency [15] significantly improves the modeling of the trigger turn-on outside the fully efficient region, as verified using data control samples. Off-line, events containing identified electrons or muons are excluded and $\not\!\!E_T > 35$ GeV is required after correcting measured jet energies for instrumental effects [16]. Events with two or three high-E_T jets are selected, and the two jets with the largest transverse energies $E_T^{j_1}$ and $E_T^{j_2}$ are required to satisfy $25 < E_T^{j_1} < 200$ GeV and $20 < E_T^{j_2} < 120$ GeV, where the jet energies are determined from calorimeter deposits corrected by track momentum measurements [17]. Some of these events consist of single-top-quark candidates in which the tau lepton from the $t \to Wb \to \tau\nu b$ decay is reconstructed as a jet in the calorimeters. To increase the acceptance for events with an unidentified τ lepton, events in which the third-most energetic jet satisfies $15 < E_T^{j_3} < 100$ GeV are accepted. Because of the large rate of inclusive quantum chromodynamics (QCD) multijet (MJ) production, events with four or more reconstructed jets, where each jet has transverse energy in excess of 15 GeV and pseudorapidity [11] $|\eta| < 2.4$, are rejected. To ensure that the two leading-E_T jets are within the silicon-detector acceptance, they are required to satisfy $|\eta| < 2$, with at least one of them satisfying $|\eta| < 0.9$.

The MJ background events most often contain $\not\!\!E_T$ generated through jet energy mismeasurements. Neutrinos produced in semileptonic b-hadron decays can also contribute to the $\not\!\!E_T$ of these events. In both cases, the $\vec{\not\!\!E}_T$ is typically aligned with $\vec{E}_T^{j_2}$, and events are rejected by requiring the azimuthal separation between $\vec{\not\!\!E}_T$ and $\vec{E}_T^{j_2}$ (or $\vec{E}_T^{j_3}$, for events with a third jet) to be larger than 0.4. The remaining MJ background has a large contribution of events with jets from fragmenting light-flavored u, d, and s quarks or gluons, which can be further reduced by requiring b-tagged jets. Charm quarks, which share some features associated with b quarks, are not explicitly identified. Events are assigned to three independent subsamples depending on the b-tag output of the two leading jets. Jets with b-tag values larger than 0.98 are defined as tightly tagged (T jet), whereas jets with outputs between 0.72 and 0.98 are defined as loosely tagged (L jet). The tagging efficiency and misidentification rate applied to each jet depend on the jet E_T and η. Scale factors for these variables are applied on a per-jet basis to bring the b-tagging efficiencies in the simulation into agreement with those in the data. TT events are defined as those in which both jets are tightly tagged, TL events as those in which one jet is tightly tagged and the other is loosely tagged, and $1T$ events as those in which only one jet is tightly tagged while the other is untagged. Events with two and three jets are analyzed separately, leading to six event subsamples with differing signal-to-background ratios. This strategy enhances sensitivity and helps separate s-channel single-top-quark production enhanced in the double-tag categories from the t-channel production enhanced in the single-tag categories.

In order to extract the s-channel electroweak single-top-quark signal from the more dominant background contributions, the rates and kinematic distributions of events associated with each process need to be accurately modeled. The kinematic distributions of events associated with top-quark-pair, single-top-quark, $V+$jets (where V stands for a W or a Z boson), $W+c$, diboson (VV), and associated Higgs and W or Z boson (VH) production are modeled using simulations. The ALPGEN generator [18,19] is used to model $V+$jets at leading order (LO) with up to four partons based on generator-to-reconstructed-jet matching [20,21] and $W+c$. The POWHEG [22] generator is used to model t- and s-channel single-top-quark production, while PYTHIA [23] is used to model top-quark-pair, VV, and VH production at LO. Each of the event generators uses the CTEQ5L parton distribution function [24] as input to the simulations. Parton showering is simulated in all cases using PYTHIA tuned to the Tevatron underlying-event data [25]. Event modeling also includes simulation of the detector response using GEANT [26]. The simulated events are reconstructed and analyzed in the same way as the experimental data. Normalizations of the event contributions from t-channel single-top-quark, VV, VH, and $t\bar{t}$ pair production are taken from theoretical-cross-section predictions [27–30], while normalization for $W+c$ production is taken from the measured cross section [31]. For $V+$jets production, the heavy-flavor contribution is normalized based on the number of b-tagged events observed in an independent data control sample [32]. Contributions of $V+$jets and VV events containing at least one incorrectly b-tagged, light-flavored jet are determined by applying per-event mistag probabilities obtained from a generic event sample containing light-flavored jets [33] to simulated events. The MJ background [13] remaining after the full selection criteria is modeled by applying a tag-rate matrix derived from a MJ-dominated data sample to events in an inclusive sample selected without b-tagging requirements (pretag events) that, otherwise, satisfy the signal sample selection criteria.

In order to separate the s-channel single-top-quark signal from the backgrounds, a staged neural network (NN) technique is employed. A first network NN_{QCD} is trained to discriminate MJ events from signal events. Events that

TABLE I. Numbers of predicted and observed two-jet events in the $1T$, TL, and TT subsamples. The uncertainties on the predicted numbers of events are due to the theoretical-cross-section uncertainties and the uncertainties on signal and background modeling. Both the uncertainties and the central values are those obtained from the fit to the data, which incorporates the theoretical constraints.

Category	$1T$	TL	TT
t-channel single top	161 ± 31	10.8 ± 2.1	9.2 ± 1.7
$t\bar{t}$	243 ± 24	84.8 ± 9.3	92.4 ± 8.4
Diboson	285 ± 26	51.3 ± 4.6	37.2 ± 3.4
VH	12.6 ± 1.4	6.6 ± 0.8	7.6 ± 0.8
$V+$jets	6528 ± 2048	694 ± 216	220 ± 69
MJ	8322 ± 180	928 ± 59	300 ± 32
Signal	86.2 ± 47.7	41.8 ± 23.2	45.9 ± 25.3
Total prediction	15557 ± 2056	1733 ± 224	663 ± 76
Observed	15312	1743	686

TABLE II. Numbers of predicted and observed three-jet events in the $1T$, TL, and TT subsamples.

Category	$1T$	TL	TT
t-channel single top	82.2 ± 15.8	7.5 ± 1.5	6.8 ± 1.3
$t\bar{t}$	597 ± 60	118 ± 13	110 ± 10
Diboson	108 ± 10	15.7 ± 1.5	8.8 ± 0.8
VH	6.0 ± 0.7	1.9 ± 0.2	2.2 ± 0.2
$V+$jets	1610 ± 505	165 ± 51	50 ± 16
MJ	1818 ± 49	188 ± 15	55.9 ± 7.6
Signal	45.7 ± 25.3	15.4 ± 8.5	16.2 ± 8.9
Total prediction	4220 ± 511	495 ± 55	234 ± 20
Observed	4198	490	237

satisfy a minimal requirement on the $\mathrm{NN_{QCD}}$ output variable are further analyzed by a function $\mathrm{NN_{sig}}$ derived from the outputs of two additional NNs, $\mathrm{NN}_{V\mathrm{jets}}$ and $\mathrm{NN}_{t\bar{t}}$, designed, respectively, to separate the signal from $V+$jets (and the remaining MJ events) and $t\bar{t}$ backgrounds.

The $\mathrm{NN_{QCD}}$ discriminant is trained using MJ data events for the background sample. Since the kinematic properties associated with the presence of a W boson in the s-channel single-top-quark and $W+$jets production processes are very similar, in contrast with those of events originating from MJ production, $W+$jets events are used for the signal sample. The discriminant is trained separately for the two-jet and three-jet samples using 12 to 15 kinematic, angular, and event-shape quantities for the input variables. By requiring a threshold on $\mathrm{NN_{QCD}}$, the multijet contribution is reduced by 88% while keeping 85% of the signal. The observed and estimated event yields after the $\mathrm{NN_{QCD}}$ requirement are shown in Tables I and II.

The two additional networks $\mathrm{NN}_{V\mathrm{jets}}$ and $\mathrm{NN}_{t\bar{t}}$ are trained for events that satisfy the minimum requirement on the $\mathrm{NN_{QCD}}$ output variable. The first $\mathrm{NN}_{V\mathrm{jets}}$ is trained to separate the s-channel single-top-quark signal from $V+$jets and the remaining MJ backgrounds. In the training, a simulated signal is used, while the background sample consists of pretag data events that satisfy the requirement on $\mathrm{NN_{QCD}}$ reweighted by the probability for an event to be b tagged (tag-rate probability) as derived from the tag-rate matrix. The $\mathrm{NN_{QCD}}$ requirement changes the pretag data composition, enhancing the $V+$jets contribution and selecting MJ events with properties closer to those expected for $V+$jets events. The background model obtained by reweighting these events via the tag-rate probability accounts for both the $V+$jets and MJ event contributions, allowing for more straightforward training of the $\mathrm{NN}_{V\mathrm{jets}}$. The second $\mathrm{NN}_{t\bar{t}}$ is trained to separate the s-channel single-top-quark from $t\bar{t}$ production using simulation for both components. Variables which describe the energy and momentum flow in the detector and angular variables are used in the training of the $\mathrm{NN}_{V\mathrm{jets}}$ and $\mathrm{NN}_{t\bar{t}}$ discriminants. The final discriminant $\mathrm{NN_{sig}}$ is defined as the quadrature sum of the $\mathrm{NN}_{V\mathrm{jets}}$ and $\mathrm{NN}_{t\bar{t}}$ output variables, both weighted by an appropriate weight optimized to improve the sensitivity in each analysis subsample, taking into account the differing background contributions. Figure 2 shows the predicted and observed shapes of the $\mathrm{NN_{sig}}$ output variable for each of the six event subsamples.

The modeling of SM backgrounds is tested in several control samples. A first (EWK) control sample is defined containing events with at least one charged lepton that, otherwise, satisfy the selection criteria. This sample is independent from the signal sample and is sensitive primarily to top-quark-pair, $V+$jets, and, to a lesser extent, VV production. A second (QCD) control sample contains events that do not meet the minimal requirement on the $\mathrm{NN_{QCD}}$ output variable but, otherwise, satisfy the selection criteria. This event sample dominated by MJ production is used to validate the data-driven MJ background model and obtain scale factors ranging from 0.7 to 0.9 for normalizing modeled contributions to the TT, TL, and $1T$ event subsamples. Comparisons of modeled and observed distributions for multiple kinematic variables, including those used as inputs to the $\mathrm{NN_{QCD}}$, $\mathrm{NN}_{V\mathrm{jets}}$, and $\mathrm{NN}_{t\bar{t}}$ are used to validate the accuracy of the model.

To measure the signal contribution, the sum of contributions to the $\mathrm{NN_{sig}}$ distribution is fitted to the observed data, accounting for statistical and systematic uncertainties. The dominant systematic uncertainties arise from the normalization of the $V+$heavy-flavor background contributions (30%), differences in b-tagging efficiencies between the data and simulation (8%–16%), and mistag rates (20%–30%) [14]. Other uncertainties are on the $t\bar{t}$ (3.5%), t-channel single-top-quark (6.2%), VV (6%), VH (5%), and $W+c$ (23%) cross sections [27–31], initial- and final-state radiation (2%), normalizations of the QCD multijet background (3%–7%), luminosity measurement (6%) [34], jet-energy scale (1%–6%) [16], trigger

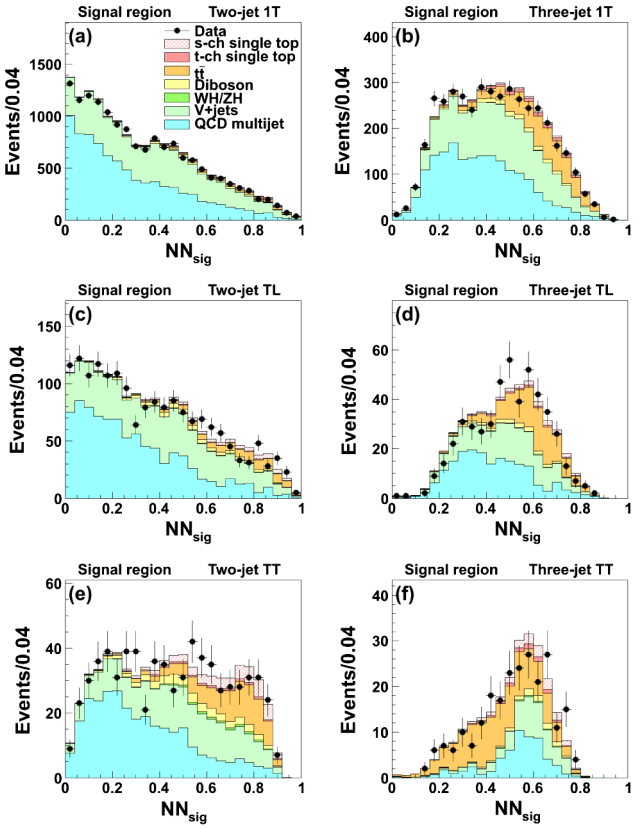

FIG. 2 (color online). Predicted and observed final discriminant distributions in the signal region for (a) $1T$ two-jet, (b) $1T$ three-jet, (c) TL two-jet, (d) TL three-jet, (e) TT two-jet, and (f) TT three-jet event subsamples.

efficiency (1%–3%), parton distribution functions (2%), and lepton vetoes (2%). The shapes obtained by varying the tag-rate probabilities by 1 standard deviation from their central values are applied as uncertainties on the shapes of the $\mathrm{NN_{sig}}$ output distribution for the MJ background. Changes in the shape of the $\mathrm{NN_{sig}}$ distribution originating from jet energy scale uncertainties are also incorporated for processes modeled via the simulation.

A likelihood fit to the binned $\mathrm{NN_{sig}}$ distribution is used to extract the s-channel single-top-quark signal in the presence of SM backgrounds. The likelihood is the product of Poisson probabilities over the bins of the final discriminant distribution. The mean number of expected events in each bin includes contributions from each background source and s-channel single-top-quark production, assuming a top-quark mass of 172.5 GeV/c^2. To extract the signal cross section, a Bayesian method is employed [35]. A uniform prior probability in the non-negative range for the s-channel single-top-quark-production cross section times branching fraction and truncated Gaussian priors for the uncertainties on the acceptance and shape of each process are incorporated in the fit. Results from each of the six search subsamples are combined by taking the product of their likelihoods and simultaneously varying the correlated uncertainties.

The measured s-channel single-top-quark cross section in the $\not{E}_T b\bar{b}$ sample is $1.12^{+0.61}_{-0.57}$ (stat + syst) pb. The probability of observing a signal as large as the observed one or larger that results from fluctuations of the background (p value) is determined using pseudoexperiments to be 3.1×10^{-2}, corresponding to a significance of 1.9 standard deviations. The median expected significance assuming that a signal is present at the SM rate is 1.8 standard deviations.

This result is combined with the result of a similar search in the $\ell\nu b\bar{b}$ sample [12]. In that search, candidate events were selected by requiring exactly one reconstructed muon or electron in the final state. Hence, no such events are included in the $\not{E}_T b\bar{b}$ analysis described above. Four independent tagging categories, according to the score of the HOBIT tagger on the two leading jets (tight tight TT, tight loose TL, single tight $1T$, and loose loose LL) were analyzed separately. Events were also divided into three independent samples based on different categories of reconstructed leptons. To further discriminate the signal from all other backgrounds, neural networks were employed. These NNs were optimized separately for each tagging and lepton category. Correlated systematic uncertainties were treated as described above for the $\not{E}_T b\bar{b}$ search. Finally, a binned-likelihood technique was applied to the final NN output to extract the s-channel single-top-quark cross section. The significance of the result from the $\ell\nu b\bar{b}$ channel was 3.8 standard deviations, and the measured cross section was $1.41^{+0.44}_{-0.42}$ (stat + syst) pb, assuming a top-quark mass of 172.5 GeV/c^2.

The two analyses are combined by taking the product of their likelihoods and simultaneously varying the correlated uncertainties, following the same procedure explained above. The uncertainties associated with the theoretical cross sections of the $t\bar{t}$, t-channel electroweak single-top-quark, VV, and VH production processes, the luminosity, the b-tagging efficiency, and the mistag rate are considered fully correlated between the two searches. The combined measurement results in an s-channel single-top-quark-production cross section of $1.36^{+0.37}_{-0.32}$ pb, consistent with the SM cross section of 1.05 ± 0.05 pb [28]. The combined background-only p value is 1.6×10^{-5}, which corresponds to a signal significance of 4.2 standard deviations. The median expected significance is 3.4 standard deviations.

In summary, we perform for the first time a search for s-channel single-top-quark production in the $\not{E}_T b\bar{b}$ channel. The result is combined with that of a search in the $\ell\nu b\bar{b}$ channel [12] to strengthen the reported evidence for s-channel single-top-quark production, leading to an improvement of more than 10% on the uncertainty of the measured cross section.

We thank the Fermilab staff and the technical staffs of the participating institutions for their vital contributions. This work was supported by the U.S. Department of Energy and

National Science Foundation, the Italian Istituto Nazionale di Fisica Nucleare, the Ministry of Education, Culture, Sports, Science and Technology of Japan, the Natural Sciences and Engineering Research Council of Canada, the National Science Council of the Republic of China, the Swiss National Science Foundation, the A. P. Sloan Foundation, the Bundesministerium für Bildung und Forschung, Germany, the Korean World Class University Program, the National Research Foundation of Korea, the Science and Technology Facilities Council and the Royal Society, United Kingdom, the Russian Foundation for Basic Research, the Ministerio de Ciencia e Innovación, and Programa Consolider-Ingenio 2010, Spain, the Slovak R&D Agency, the Academy of Finland, the Australian Research Council (ARC), and the EU community Marie Curie Fellowship Contract No. 302103.

[a]Deceased.
[b]Visitor from University of British Columbia, Vancouver, BC V6T 1Z1, Canada.
[c]Visitor from Istituto Nazionale di Fisica Nucleare, Sezione di Cagliari, 09042 Monserrato (Cagliari), Italy.
[d]Visitor from University of California Irvine, Irvine, CA 92697, USA.
[e]Visitor from Institute of Physics, Academy of Sciences of the Czech Republic, 182 21, Czech Republic.
[f]Visitor from CERN, CH-1211 Geneva, Switzerland.
[g]Visitor from Cornell University, Ithaca, NY 14853, USA.
[h]Visitor from University of Cyprus, Nicosia CY-1678, Cyprus.
[I]Visitor from Office of Science, U.S. Department of Energy, Washington, DC 20585, USA.
[j]Visitor from University College Dublin, Dublin 4, Ireland.
[k]Visitor from ETH, 8092 Zürich, Switzerland.
[l]Visitor from University of Fukui, Fukui City, Fukui Prefecture, Japan 910-0017.
[m]Visitor from Universidad Iberoamericana, Lomas de Santa Fe, México, C.P. 01219, Distrito Federal.
[n]Visitor from University of Iowa, Iowa City, IA 52242, USA.
[o]Visitor from Kinki University, Higashi-Osaka City, Japan 577-8502.
[p]Visitor from Kansas State University, Manhattan, KS 66506, USA.
[q]Visitor from Brookhaven National Laboratory, Upton, NY 11973, USA.
[r]Visitor from Queen Mary, University of London, London, E1 4NS, United Kingdom.
[s]Visitor from University of Melbourne, Victoria 3010, Australia.
[t]Visitor from Muons, Inc., Batavia, IL 60510, USA.
[u]Visitor from Nagasaki Institute of Applied Science, Nagasaki 851-0193, Japan.
[v]Visitor from National Research Nuclear University, Moscow 115409, Russia.
[w]Visitor from Northwestern University, Evanston, IL 60208, USA.
[x]Visitor from University of Notre Dame, Notre Dame, IN 46556, USA.
[y]Visitor from Universidad de Oviedo, E-33007 Oviedo, Spain.
[z]Visitor from CNRS-IN2P3, Paris, F-75205 France.
[aa]Visitor from Universidad Tecnica Federico Santa Maria, 110v Valparaiso, Chile.
[bb]Visitor from The University of Jordan, Amman 11942, Jordan.
[cc]Visitor from Universite catholique de Louvain, 1348 Louvain-La-Neuve, Belgium.
[dd]Visitor from University of Zürich, 8006 Zürich, Switzerland.
[ee]Visitor from Massachusetts General Hospital, Boston, MA 02114 USA.
[ff]Visitor from Harvard Medical School, Boston, MA 02114 USA.
[gg]Visitor from Hampton University, Hampton, VA 23668, USA.
[hh]Visitor from Los Alamos National Laboratory, Los Alamos, NM 87544, USA.
[ii]Visitor from Università degli Studi di Napoli Federico I, I-80138 Napoli, Italy.

[1] F. Abe *et al.* (CDF Collaboration), Phys. Rev. Lett. **74**, 2626 (1995).
[2] S. Abachi *et al.* (D0 Collaboration), Phys. Rev. Lett. **74**, 2632 (1995).
[3] T. M. P. Tait and C. P. Yuan, Phys. Rev. D **63**, 014018 (2000).
[4] T. Aaltonen *et al.* (CDF Collaboration), Phys. Rev. Lett. **103**, 092002 (2009).
[5] V. M. Abazov *et al.* (D0 Collaboration), Phys. Rev. Lett. **103**, 092001 (2009).
[6] CDF and D0 Collaboration, Tevatron Electroweak Working Group, arXiv:0908.2171.
[7] V. Abazov *et al.* (D0 Collaboration), Phys. Lett. B **705**, 313 (2011).
[8] G. Aad *et al.* (ATLAS Collaboration), Phys. Lett. B **717**, 330 (2012).
[9] S. Chatrchyan *et al.* (CMS Collaboration), J. High Energy Phys. 12 (2012) 035.
[10] V. M. Abazov *et al.* (D0 Collaboration), Phys. Lett. B **726**, 656 (2013).
[11] CDF uses a cylindrical coordinate system with the z axis along the proton beam axis. The pseudorapidity is $\eta = -\ln(\tan(\theta/2))$, where θ is the polar angle, and φ is the azimuthal angle, while $p_T = p\sin\theta$ and $E_T = E\sin\theta$. The E_T is defined as the magnitude of $\vec{E}_T = -\sum_i E_T^i \hat{n}_i$, where $\hat{n}_i$ is a unit vector perpendicular to the beam axis and pointing at the ith calorimeter tower, and E_T^i is the transverse energy therein.
[12] T. Aaltonen *et al.* (CDF Collaboration), Phys. Rev. Lett. **112** 231804 (2014).
[13] T. Aaltonen *et al.* (CDF Collaboration), Phys. Rev. D **87**, 052008 (2013).
[14] J. Freeman, T. Junk, M. Kirby, Y. Oksuzian, T. J. Phillips, F. D. Snider, M. Trovato, J. Vizan, and W. M. Yao, Nucl. Instrum. Methods Phys. Res., Sect. A **697**, 64 (2013).
[15] K. Potamianos, Ph. D. thesis, Purdue University [Report No. FERMILAB-THESIS-2011-34, 2011].

[16] A. Bhatti *et al.*, Nucl. Instrum. Methods Phys. Res., Sect. A **566**, 375 (2006).
[17] C. Adloff *et al.* (H1 Collaboration), Z. Phys. C **74**, 221 (1997).
[18] M. L. Mangano, M. Moretti, F. Piccinini, R. Pittau, and A. D. Polosa, J. High Energy Phys. 07 (2003) 001.
[19] The factorization and renormalization scale in the ALPGEN samples are both set to be $\sqrt{M_W^2 + \sum_{\text{partons}} m_T^2}$, where $m_T^2 = m^2 + p_T^2/c^2$. For light-flavored partons, m is zero, while for b quarks, $m = 4.7$ GeV/c^2, and for c quarks, $m = 1.5$ GeV/c^2.
[20] M. L. Mangano, M. Moretti, F. Piccinini, and M. Treccani, J. High Energy Phys. 01 (2007) 013.
[21] J. Alwall, S. Hoche, F. Krauss, N. Lavesson, L. Lonnblad, F. Maltoni, M. Mangano, M. Moretti, C. Papadopoulos, F. Piccinini, S. Schumann, M. Treccani, J. Winter, and M. Worek, Eur. Phys. J. C **53**, 473 (2008).
[22] S. Alioli, P. Nason, C. Oleari, and E. Re, J. High Energy Phys. 06 (2010) 043.
[23] T. Sjostrand, S. Mrenna, and P. Skands, J. High Energy Phys. 05 (2006) 026.
[24] H. Lai, J. Huston, S. Kuhlmann, J. Morfin, F. Olness, J. Owens, J. Pumplin, and W. Tung, Eur. Phys. J. C **12**, 375 (2000).
[25] T. Aaltonen *et al.* (CDF Collaboration), Phys. Rev. D **82**, 034001 (2010).
[26] GEANT, detector description and simulation tool, CERN Program Library Long Writeup Report No. W5013, 1993.
[27] P. Bärnreuther, M. Czakon, and A. Mitov, Phys. Rev. Lett. **109**, 132001 (2012).
[28] N. Kidonakis, Phys. Rev. D **81**, 054028 (2010).
[29] J. M. Campbell and R. K. Ellis, Phys. Rev. D **60**, 113006 (1999).
[30] J. Baglio and A. Djouadi, J. High Energy Phys. 10 (2010) 064; O. Brien, R. V. Harlander, M. Weisemann, and T. Zirke, Eur. Phys. J. C **72**, 1868 (2012).
[31] T. Aaltonen *et al.* (CDF Collaboration), Phys. Rev. Lett. **110**, 071801 (2013).
[32] T. Aaltonen *et al.* (CDF Collaboration), Phys. Rev. D **82**, 112005 (2010).
[33] D. Acosta *et al.* (CDF Collaboration), Phys. Rev. D **71**, 052003 (2005); A. Abulencia *et al.* (CDF Collaboration), Phys. Rev. D **74**, 072006 (2006).
[34] S. Klimenko, J. Konigsberg, and T. M. Liss, Report No. FERMILAB-FN-0741, 2003.
[35] K. Nakamura (Particle Data Group), J. Phys. G **37**, 075021 (2010).